AGU PUBLICATIONS

Geochemistry, Geophysics, Geosystems

RESEARCH ARTICLE
10.1002/2016GC006396

Key Points:
- A comparison of paleointensity results determined with different techniques has been performed on historical and Pleistocene lavas
- Results on historical flows suggest that agreement between both methods is a good indicator of correct paleointensity determinations
- No clear relation between correct or anomalous paleointensity results and their determination quality or rock-magnetic properties

Supporting Information:
- Figure S1

Correspondence to:
M. Calvo-Rathert,
mcalvo@ubu.es

Citation:
Calvo-Rathert, M., J. Morales-Contreras, Á. Carrancho and A. Goguitchaichvili (2016), A comparison of Thellier-type and multispecimen paleointensity determinations on Pleistocene and historical lava flows from Lanzarote (Canary Islands, Spain), *Geochem. Geophys. Geosyst.*, *17*, 3638–3654, doi:10.1002/2016GC006396.

Received 12 APR 2016
Accepted 31 AUG 2016
Accepted article online 3 SEP 2016
Published online 13 SEP 2016

A comparison of Thellier-type and multispecimen paleointensity determinations on Pleistocene and historical lava flows from Lanzarote (Canary Islands, Spain)

Manuel Calvo-Rathert[1], Juan Morales-Contreras[2], Ángel Carrancho[3], and Avto Goguitchaichvili[2]

[1]Departamento de Física, Escuela Politécnica Superior, Universidad de Burgos, Burgos, Spain, [2]Laboratorio Interinstitucional de Magnetismo Natural, Instituto de Geofísica, Unidad Michoacán UNAM – Campus Morelia, Morelia, Mexico, [3]Departamento de Historia, Geografía y Comunicación, Universidad de Burgos, Burgos, Spain

Abstract Sixteen Miocene, Pleistocene, and historic lava flows have been sampled in Lanzarote (Canary Islands) for paleointensity analysis with both the Coe and multispecimen methods. Besides obtaining new data, the main goal of the study was the comparison of paleointensity results determined with two different techniques. Characteristic Remanent Magnetization (ChRM) directions were obtained in 15 flows, and 12 were chosen for paleointensity determination. In Thellier-type experiments, a selection of reliable paleointensity determinations (43 of 78 studied samples) was performed using sets of criteria of different stringency, trying to relate the quality of results to the strictness of the chosen criteria. Uncorrected and fraction and domain-state corrected multispecimen paleointensity results were obtained in all flows. Results with the Coe method on historical flows either agree with the expected values or show moderately lower ones, but multispecimen determinations display a large deviation from the expected result in one case. No relation can be detected between correct or anomalous results and paleointensity determination quality or rock-magnetic properties. However, results on historical flows suggest that agreement between both methods could be a good indicator of correct determinations. Comparison of results obtained with both methods on seven Pleistocene flows yields an excellent agreement in four and disagreements in three cases. Pleistocene determinations were only accepted if either results from both methods agreed or a result was based on a sufficiently large number ($n > 4$) of individual Thellier-type determinations. In most Pleistocene flows, a VADM around 5×10^{22} Am^2 was observed, although two flows displayed higher values around 9×10^{22} Am^2.

1. Introduction

Knowledge about the characteristics and variations of the ancient Earth's magnetic field can supply information of great interest to gain a better understanding of the processes associated with the evolution of the Earth's profound interior. Paleomagnetic studies often only supply the directional information provided by the remanence vector, but a better comprehension of the characteristics and variations of the geomagnetic field also needs the information provided by the intensity of the paleofield vector. However, while paleofield directions are relatively easy to obtain as they are generally parallel to magnetization directions, determinations of the absolute paleointensity of the Earth's magnetic field are much more complicated, because the magnetization intensity recorded in rocks is not equal, but only proportional to the field strength. To date, several different methods for paleointensity determination have been used, but those based on the method originally proposed by Thellier [*Thellier and Thellier*, 1959] are deemed to be the most reliable ones to retrieve the absolute value of the field strength, as they rely on a rigorous physical background.

Through the acquisition of thermoremanent magnetisation (TRM) during their formation, volcanic rocks can carry a geologically instantaneous and accurate record of the Earth's magnetic field, allowing the retrieval of absolute paleointensity values. However, as shown by the paleointensity database PINT2015.05 [*Biggin et al.*, 2010], existing data are still limited and not uniformly distributed. The failure rate of the experiments is often large and the dispersion of paleointensity results is much higher than the scatter of standard directional results, often because erroneous determinations are regarded to depict a correct paleointensity result [e.g., *Calvo et al.*, 2002]. In Thellier-type experiments, several requirements have to be fulfilled in order for a

sample to be able to provide a reliable paleointensity determination: (i) remanence must be a thermoremanent magnetization (TRM); (ii) samples must obey the Thellier laws of reciprocity, independence, and additivity of pTRMs [*Thellier and Thellier*, 1959], a condition which is fulfilled by noninteracting single-domain (SD), but not multidomain (MD) particles [*Shaskanov and Metallova*, 1972; *Levi*, 1977; *Bol'shakov and Shcherbakova*, 1979; *Worm et al*., 1988]; (iii) irreversible chemical/mineralogical or physical changes produced during heating [e.g., *Kosterov and Prévot*, 1998] must be prevented or, at least, minimized, as they can have an effect on magnetic phases, resulting in spurious paleointensity estimates.

In recent years, new methods have been proposed to avoid or diminish problems related to chemical/mineralogical alterations during paleointensity experiments or the presence of MD grains. *Dekkers and Böhnel* [2006] have proposed a multispecimen (MS) method, which consists of the acquisition of a pTRM parallel to NRM at a specific temperature and at a chosen field on a subspecimen taken from a sample, with the experiment being repeated at the same temperature but at different fields on other subspecimens of the same sample. The field which creates a magnetization that being added to the remaining NRM equals the specimen's original NRM is supposed to have the strength of the original magnetizing field and to be more independent of domain structure, as this approach would eliminate magnetic history effects. Alteration can also be reduced by this method, as specimens are being heated only once, often to intermediate temperatures. *Fabian and Leonhardt* [2010], however, consider that application of the MS method on samples containing MD grains systematically overestimates paleointensity, and *Michalk et al*. [2008, 2010] have reported paleointensity overestimates with the MS method on lavas containing a significant MD fraction. *Fabian and Leonhardt* [2010] proposed a new MS protocol which includes a domain-state correction but requires an extra number of heatings and measurements.

Thellier-type and the MS method rely on different measurement protocols which are based on the acquisition of different energy equilibrium states related to temperature, applied field, demagnetizing field, etc., at the different experimental stages included in the experiment. Comparison of the results obtained with a Thellier-type and the MS method accompanied by detailed rock-magnetic experiments may provide useful information, especially if experiments are performed on rocks in which magnetization was acquired in a known field. In fact, consistency of paleointensity determinations obtained from methods relying on different principles may support the reliability of such results [*Böhnel et al*., 2009; *De Groot et al*., 2013, 2015; *Monster et al*., 2015a]. Furthermore, interesting information might be obtained when analyzing rock-magnetic characteristics of sites in which results obtained with both methods agree or disagree.

Absolute paleointensity data are still scarce if compared to directional paleomagnetic results, so that new successful determinations are always interesting in order to improve the existing database. Although several paleointensity studies have been carried out in the Canary Islands, none has been performed in Lanzarote. Previous paleomagnetic work in Lanzarote is also scarce [*Watkins et al*., 1966; *Soler et al*., 1984]. While in the former study no definite information about the age of the analyzed lavas is provided ("older lavas"), *Soler et al* [1984] deliver paleomagnetic results for two historical flows (1730 and 1824 A.D.).

For the reasons outlined above, in the present study, two Miocene, eight Pleistocene, and six historic lava flows have been sampled in the island of Lanzarote (Canary Islands, Spain) for rock-magnetic, paleomagnetic, and paleointensity analysis with both a Thellier-type method and the multispecimen method. Sampling was performed with a gasoline-powered portable drill and both a magnetic and a solar compass were used for sample orientation. Comparison of the measured magnetic and solar azimuth of the field correction showed that only very few individual cores produced large significant deflections from the reference field, and even these large deflections lay below 10°. At a site level, observed deviations were low, with only flow LZ5 showing a moderate 5° eastward declination anomaly. The mean of all samples with available solar azimuth data agreed exactly with the expected declination (4.6°W), thus not showing any deflection at all. Ages of nonhistorical flows (Table 1) were obtained in one case from a K-Ar dating directly performed on the sampled unit [*Coello et al*., 1992]. In the other cases, dating was based on volcano-stratigraphic information relying on available K-Ar ages in Lanzarote [*Abdel-Monem et al*., 1971; *Coello et al*., 1992].

2. Geologic Setting

Lanzarote belongs to the Canary Islands, an archipelago consisting of seven volcanic edifices situated in the eastern Atlantic Ocean, 100–700 km west of the Sahara continental margin (Figure 1). As can be estimated

Table 1. Paleomagnetic Results[a]

SITE	AGE	LAT	LON	N(n)	L+P	DEC	INC	α_{95}	k	PLAT	PLON
Historical Flows											
TM1	1824	29.01	346.25	10(10)	9 + 1	331.0	54.2	10.6	20	64.8	276.8
LZ9	1736	29.08	346.28	8(8)		356.8	56.6	11.8	23	81.5	328.9
TM3	1732/1736	28.99	346.26	9(9)		354.6	55.8	6.1	73	81.4	315.9
LZ2	1731/1732	28.99	346.17	10(11)	3 + 7	348.7	58.3	10.0	28	76.3	306.1
TM2	1731/1732	29.00	346.23	9(9)		351.7	59.0	5.1	104	77.2	136.0
TM4	1731/1732	28.99	346.26	7(8)		327.5	63.5	13.3	22	59.7	297.4
Pleistocene Flows											
LZ1	PLE (Ion)	28.99	346.17	8(8)		360.0	49.5	3.4	260	88.6	344.8
LZ4	PLE (Ion)	28.98	346.17	8(8)		359.5	42.2	3.7	229	85.4	171.8
LZ5	PLE (Ion)	28.96	346.21	8(8)		17.5	36.3	3.4	266	71.9	101.2
LZ7	PLE (Ion)	29.08	346.28	8(8)		2.0	50.3	5.3	110	87.3	27.6
LZ10	PLE (Ion)	29.12	346.34	6(6)		14.1	37.3	8.3	66	74.8	106.0
LZ12	PLE (Ion)	29.00	346.51	8(8)		15.2	38.5	3.1	311	74.5	101.2
LZ3	0.92 Myr	28.93	346.18	8(8)		358.5	33.7	5.3	110	79.4	174.1
LZ8	PLE (Cal)	29.08	346.28	6(11)	4 + 2	6.3	52.1	7.0	100	83.5	40.8
Mean (Pleistocene flows)				8		6.9	42.7	7.9	76		
Miocene Flows											
LZ6	u. MIO	28.95	346.26	7(7)		327.5	70.6	5.2	137	55.2	313.5
LZ11	lm. MIO.	28.91	346.26	No coherent results							

[a]*SITE*: flow number. *AGE*: age of the flow (LZ3: *Coello et al*. [1992]). *LAT* and *LON*: latitude and longitude of site. *N*(*n*): *N*: number of samples (specimens); in site mean calculations, N is the number of flows. (*L*+*P*): number of directly determined directions (L) and planes (P) used for calculation of flow mean. *DEC* and *INC*: declination and inclination of ChRM. α_{95}: Radius of 95% confidence cone. *k*: precision parameter. *PLAT* and *PLON*: latitude and longitude of virtual geomagnetic poles.

from the magnetic anomaly pattern of the central Atlantic, the island group formed as a result of alkaline magmas rising through a 150–175 Myr old oceanic crust [*Roest et al*., 1992]. The chronological and spatial evolution of the volcanism from east to west in the Canary Islands has led several authors to interpret their origin as produced during the eastward progression of the African plate over a mantle plume [e.g., *Schmincke*, 1973; *Morgan*, 1983; *Hoernle and Schmincke*, 1993; *Carracedo et al*., 1998], but the origin of the archipelago is still debated. *Anguita and Hernán* [2000] have proposed a so-called unifying model, partly based on the three mainly cited theories, which include hypotheses about the hot spot, propagating fractures, and uplifted blocks.

Lanzarote (846 km^2) lies at the eastern edge of the island chain. Two distinct cycles of subaerial volcanic activity have been recognized [*Coello et al*., 1992]. The first subaerial stage started during Miocene with the formation of two independent shield volcanoes and tabular successions of lavas and pyroclastics during

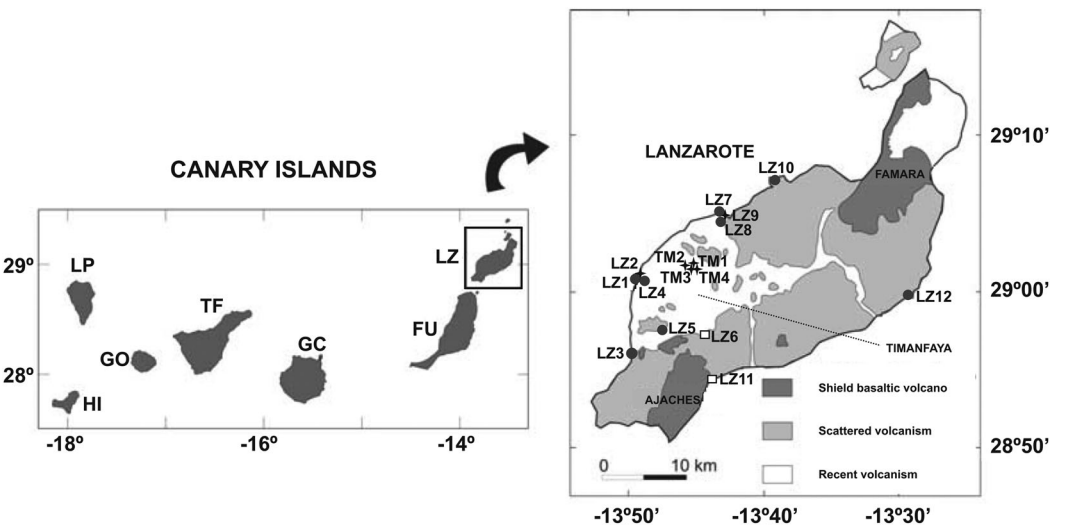

Figure 1. Map of the Canary Islands, showing the location of Lanzarote, and a simplified geological sketch of this island including sampling sites (modified from *Marinoni and Pasquarè* [1994] and *Blanco-Montenegro et al*. [2005]). LP: La Palma; H: El Hierro; G: Gomera; T: Tenerife; GC: Gran Canaria; F: Fuerteventura; LZ: Lanzarote.

upper Miocene and Pliocene [*Fúster et al*., 1968; *Carracedo and Rodríguez Badiola*, 1993]. It began in what is now the southern part of the island (Ajaches edifice, Figure 1) between 15.5 and 12.3 Ma and continued toward the North (Famara edifice, Figure 1) in three pulses between 10.2 and 3.8 Ma [*Coello et al*., 1992]. After a long period of calm, which resulted in the erosion of the Miocene edifices, volcanic activity resumed in the island with a new cycle (Figure 1) lasting from 2.7 Ma to historic times [*Coello et al*., 1992]. This cycle was characterized by fissure eruptions and the emission of basaltic lavas. From 1730 to 1736 A.D., Lanzarote suffered the longest eruption in historic times in the Canary Islands, the Timanfaya eruption (Figure 1), a basaltic-type eruption with tholeitic composition. Twenty-three percent of the island was covered in different eruptive phases, during which more than 30 volcanic cones were formed and 3–5 km^3 of materials were emitted [*Carracedo et al*., 1992]. The last eruption so far at Lanzarote Island occurred during 1824 A.D. at Tinguatón volcano.

3. Experimental Procedure

3.1. Sample Preparation

The main aim of the present study was to compare two different paleointensity determination methods and to analyze the results of successful and unsuccessful experiments in relation to the rock-magnetic properties of the analyzed samples. Therefore, a specific sample preparation was required. A 0.9 cm diameter core was drilled in the center of standard 2.54 cm diameter samples. This 0.9 cm diameter minispecimen was used for the Thellier-type paleointensity experiments. The remaining 2.54 cm diameter sample was cut into two ring-shaped specimens and one of them was cut into eight subspecimens and used for multispecimen paleointensity determinations. Nevertheless, per flow, only one (ring-shaped) sample was used for the multispecimen approach. Being taken from the same main sample and surrounding, the material used for Thellier-type paleointensity determinations should be considered as a certain guarantee that the magnetic-mineralogical composition of specimens used in both methods is the same. Remaining material from the main sample was used for rock-magnetic analysis. Other samples taken from the same core were used for directional paleomagnetic analysis.

3.2. Rock-Magnetic Experiments

The main reasons to perform rock-magnetic experiments consisted in finding out the carriers of remanence, obtaining information about their thermal stability and grain size, and as an additional criterion to appraise the suitability of the studied sites for paleointensity determinations. These experiments included the measurement of strong-field (38 mT) magnetization versus temperature (M_S-T) curves, the determination of hysteresis parameters and the recording of isothermal remanent magnetization (IRM) acquisition curves, and were carried out in the University of Burgos (Spain) with a Variable Field Translation Balance (VFTB). A first series of measurements was performed on one to three whole-rock powdered samples chosen from all flows. The following measurement sequence was applied: (i) IRM acquisition, (ii) hysteresis curve, (iii) backfield, and (iv) strong-field magnetization versus temperature (M_S-T) curve. In addition, a second series of thermomagnetic measurements was performed on all remaining samples from which specimens had been subsampled for paleointensity determination.

Hysteresis and IRM acquisition curves were recorded in a maximum applied field of approximately 1 T, and hysteresis parameters were determined from hysteresis and backfield curves. Data were analyzed with the RockMagAnalyzer 1.0 software [Leonhardt, 2006]. M_S-T curves were recorded heating samples in air up to 600 or 700°C and cooling them down to room temperature.

3.3. Paleomagnetic Measurements

Paleomagnetic measurements were carried out with a superconducting 2G magnetometer at the paleomagnetic laboratory of the University of Burgos. Initially two pilot specimens were selected from each flow for thermal demagnetization and two for alternating field (AF) demagnetization. Subsequently, the most suitable demagnetization technique was chosen for each flow. Principal component analysis [*Kirschvink*, 1980] was used to calculate the directions of remanence components and the results obtained were analyzed with the Remasoft software [*Chadima and Hrouda*, 2006].

3.4. Paleointensity Determinations

Two different methods were used for absolute paleointensity determination. One set of experiments was carried out at the University of Burgos using a Thellier-type double heating method [*Thellier and Thellier*, 1959] as modified by *Coe* [1967]. Small (0.9 cm diameter) specimens subsampled from oriented standard samples as previously described were employed for the experiments. Heating and cooling was performed in an ASC TD-48 paleointensity oven in argon atmosphere for avoiding or at least lessening oxidation. After having reached the programmed temperature in each heating step, samples were kept for some minutes at that peak temperature and subsequently the oven was turned off allowing the samples to cool down naturally during several hours. The laboratory field was left switched on for in-field steps during the whole heating-cooling procedure. The experiment was carried out in 12 temperature steps between room temperature and 582°C. After the third heating step at 216°C, pTRM-checks were performed after all but one heating step.

A second set of paleointensity experiments was performed with the multispecimen method proposed by *Dekkers and Böhnel* [2006] at the paleomagnetic laboratory of UNAM in Morelia (Mexico) using one sample per flow. Two samples (sites LZ4 and LZ5) were subjected to the original procedure [*Dekkers and Böhnel*, 2006], and in the remaining 10 cases, the extended protocols for fraction correction (FC) and domain-state correction (DSC), proposed by *Fabian and Leonhardt* [2010], were applied. The multispecimen method was carried out at a temperature of 450°C on subspecimens obtained from twelve 2.54 cm diameter ring-shaped specimens from samples used for the Thellier experiments. These ring-shaped specimens were cut into eight subspecimens and pressed into salt pellets in order to obtain standard-dimension cylindrical paleomagnetic specimens. Experiments were performed using laboratory fields from 10 to 70 μT, with increments of 10 μT. The following measurement sequence was applied to samples subjected to the extended protocol: (i) measurement of NRM; (ii) samples were oriented in such way that the natural remanent magnetization (NRM) directions of each subspecimen lay parallel to the axis of the heating chamber and were heated at 450°C in a laboratory field with this axial direction, and then their remanences were measured; (iii) specimens were set and heated as in the previous step but inverting the laboratory field direction. Then their remanences were measured; (iv) Specimens were reheated in zero field and their remanences measured. (v) Step (ii) was repeated. Before remanence measurement, a weak 5 mT AF demagnetization step was applied to erase viscous magnetization in all remanence measurements. All calculations (relative differences between pTRMs and NRMs) and corresponding correction factors are described in *Fabian and Leonhardt* [2010]. Calculations were performed by means of the VBA software implemented by *Monster et al*. [2015b]. In both sites, subjected to the original protocol of *Dekkers and Böhnel* [2006], only the first two steps were applied.

4. Paleomagnetic and Rock-Magnetic Results

4.1. Paleomagnetic Results

In most cases, samples displayed only a single main paleomagnetic component, often together with an initial weak overprint (Figures 2a and 2b). The latter could be removed at temperatures/fields below 300°C/15 mT. In a few samples, however, this viscous component appeared to be rather strong, showing an intensity comparable to the characteristic remanent magnetization (ChRM) component (Figure 2c). In three other flows (LZ2, LZ5, and LZ8), some or all samples displayed a strong secondary component, which in two of them appeared more or less overlapped with the ChRM component, so that remagnetization circle analysis had to be used in several cases. It is noteworthy that flow LZ2, which was emitted in a historical eruption in the eighteenth century, is characterized by the presence of a strong viscous component. Table 1 displays mean ChRM directions, which could be determined for each site except Miocene flow LZ11, which yielded no coherent results. All display a normal polarity direction. Paleomagnetic results from the historic flows were compared with expected directions (Figure 3) calculated with global model SHA.DIF.14k [*Pavón-Carrasco et al*., 2014], which is based on a large amount of archeomagnetic and paleomagnetic directions from lava flows compiled in the updated Geomagia50.v2 database [*Donadini et al*., 2006; *Korhonen et al*., 2008]. The expected directions obtained are D = 351°, I = 60° (1731/1732 A.D.); D = 350°, I = 60° (1736 A.D.); and D = 341°, I = 56° (1824 A.D.). Directions from all historical sites agree with the expected ones (Figure 3). In the case of site TM4, however, the mean declination shows a relatively large difference with the expected one, although the angular difference between both directions is smaller than the α_{95} value obtained for

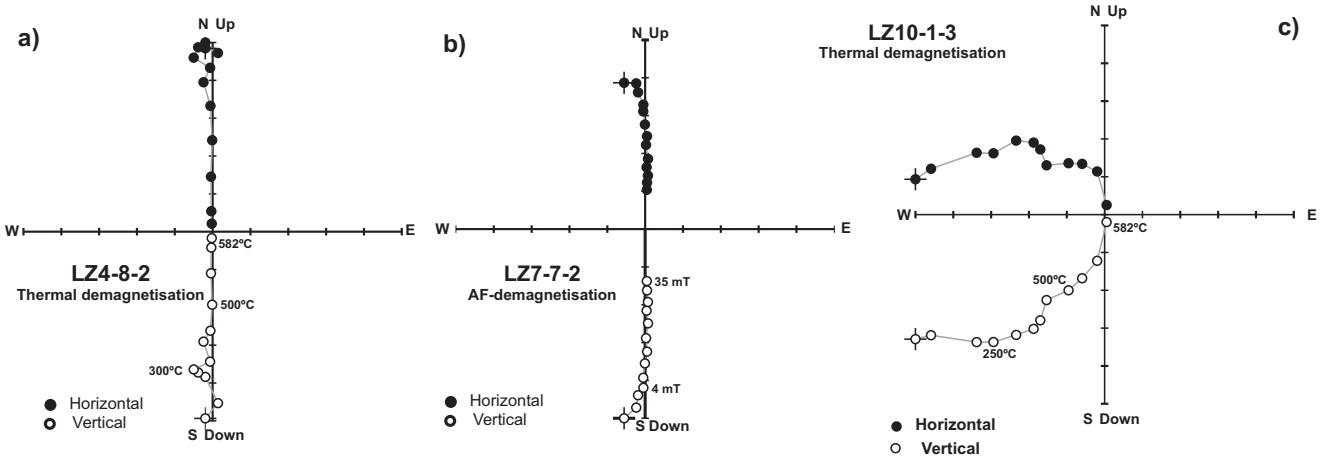

Figure 2. Orthogonal demagnetization vector plots. (a) Thermal demagnetization of LZ4-8-2. (b) AF-demagnetization of LZ7-7-2. (c) Thermal-demagnetization of LZ10-1-3. Solid symbols are for the horizontal and open symbols for the vertical projection.

that site. The mean of all Pleistocene directions agrees with the expected direction obtained from a geocentric axial dipole (Figure 3). The only available Miocene direction, however, shows a significant disagreement with the one obtained from the 10 Ma window of the synthetic apparent polar wander path for Africa (Figure 3) from *Besse and Courtillot* [2002]. This is not surprising, as the effect of secular variation is included in this direction obtained from a single volcanic flow.

4.2. Thermomagnetic Curves

The two-tangent method [*Grommé et al.*, 1969] was used to determine Curie points (T_C) of M_S-T curves. Mainly three different kinds of behavior could be recognized. Type H samples (60% of all analyzed samples, Figure 4a) displayed reversible curves with a single ferromagnetic phase characterized by a high Curie temperature between approximately 500°C and 575°C, which matches low-Ti titanomagnetite or slightly Al-substituted or Mg-substituted magnetite. Samples were regarded as being of type H when besides showing the same phases in both heating and cooling curves, the difference between initial magnetization at the start of the experiment and final magnetization at the end lay always below ±20%. In most samples from historical flows TM1 and TM3, this kind of curves could also be found, but showing considerably lower Curie temperatures between 450°C and 500°C (Figure 4b). In one case, T_C was even as low as 418°C, which would correspond to titanomagnetite with a moderate but not low Ti-fraction ($x \approx 0.3$). Nevertheless, in some sites, it could be observed that Curie temperatures from type H heating curves were somewhat higher (10–50°C) than those from the cooling curve. We do not think that this disagreement

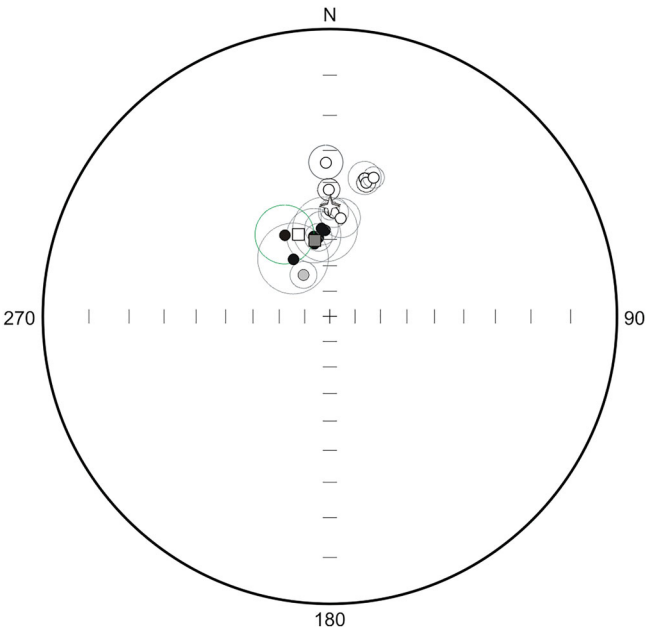

Figure 3. Stereographic projection of mean directions (circles) and 95% confidence cones of historical (solid circles), Pleistocene (open circles), and Miocene (grey circle) flows from Lanzarote. A grey star shows the expected direction corresponding to the 10 Ma window of the African synthetic polar wander path of *Besse and Courtillot* [2002] and a white star the expected Pleistocene direction, calculated from a geocentric axial dipole. Expected directions for historical flows are shown with a grey square (1730–1736 A.D. eruptions) and a white square (1824 A.D. eruption).

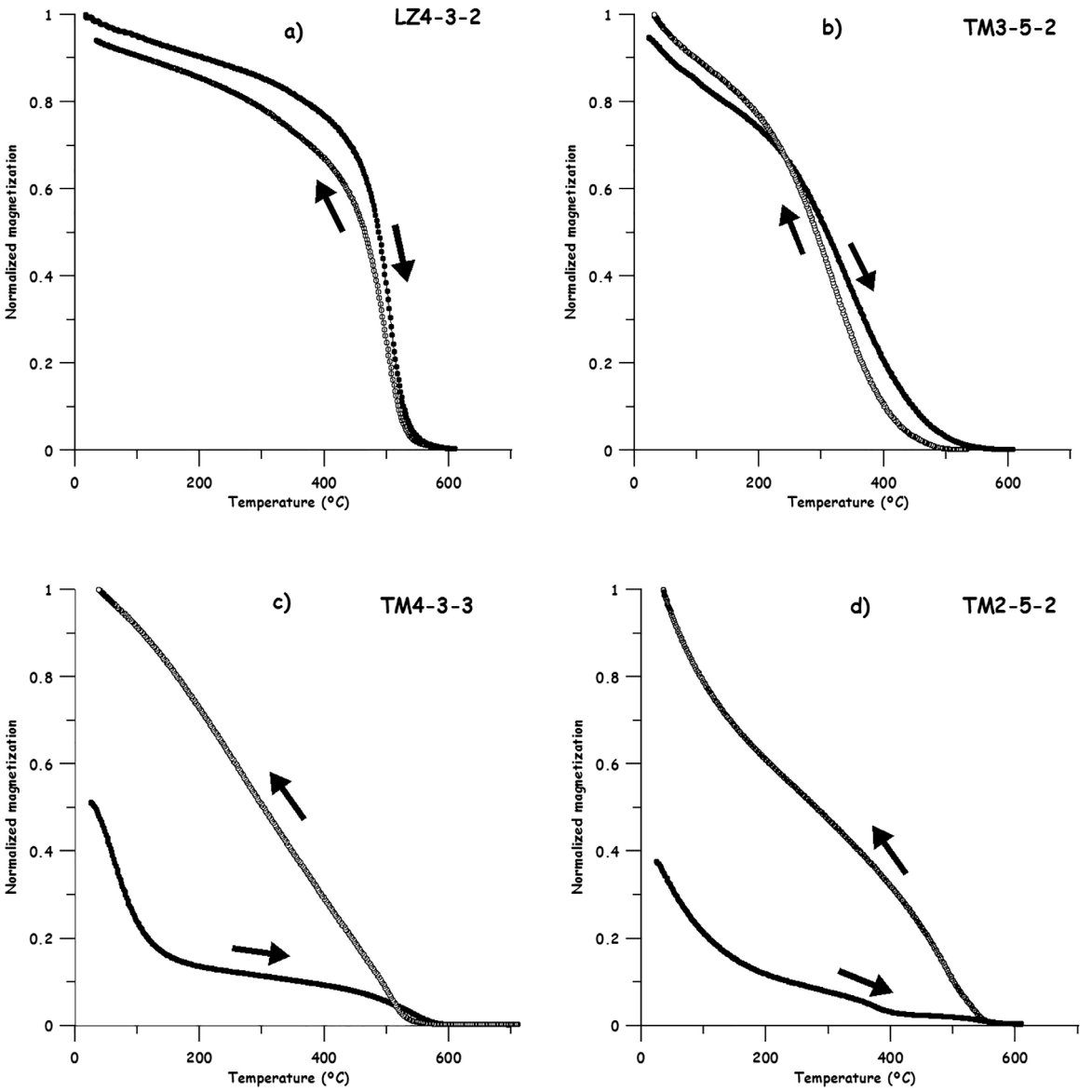

Figure 4. Normalized strong field magnetization-versus-temperature curves from lava flow samples from Lanzarote. (a) Type H curve. Sample LZ4-3-2. (b) Type H curve. Sample TM3-5-2. (c) Type L curve. Sample TM4-3-3. (d) Type M curve. Sample TM2-5-2.

is due to a difference between the recorded and the real specimen temperature, because the temperature increase and decrease rate was set at a moderate rate of 20°C per minute and the specimens were powdered, thus displaying a large effective surface for heating and cooling. Changes in Curie temperature, however, can also arise from cation reordering during heating in thermomagnetic experiments [*Bowles et al.*, 2013]. On the other hand, type H samples displaying highest Curie temperatures around or below 500°C in the heating curve often showed slightly increased (10–30°C) highest Curie temperatures in the cooling curves.

Type L samples (29% of all analyzed samples, Figure 4c) were characterized by irreversible thermomagnetic curves with a low Curie temperature (between 70°C and 250°C) and often a high Curie temperature phase (between 500°C and 575°C), in both the heating and the cooling curve. Often the low T_C phase appeared less pronounced or was absent (site LZ6) in the cooling curve. The low-temperature phase would correspond to titanomagnetite characterized by rather high titanium content ($x \approx 0.5–0.7$), and the high-temperature phase to low-Ti titanomagnetite.

Ten percent of the analyzed samples belonged to irreversible type M samples (Figure 4d), characterized by the presence of a low Curie temperature phase (between 60°C and 260°C) and an intermediate to high Curie temperature phase (between 350°C and 520°C) in the heating curve, which in some cases was accompanied by a very weak magnetite fraction. In the cooling curve, a high T_C-phase (low-Ti titanomagnetite) and in some cases a low Curie temperature phase were observed. This type of curve was mainly found in historic lava flow TM2.

4.3. IRM Acquisition and Hysteresis Experiments

In IRM acquisition curves, applied fields smaller than 200 mT were able to produce more than 90% of saturation magnetization. Thus, these measurements indicate that low-coercivity phases are the main carriers of remanence.

Hysteresis and backfield curves supplied hysteresis parameters such as M_S (saturation magnetization), M_{RS} (saturation remanence), B_C (coercivity), and B_{CR} (coercivity of remanence). Hysteresis parameter ratios display a PSD (pseudo single-domain) behavior, as shown in the Day-plot [*Day et al*., 1977] in supporting information Figure S1a. This behavior can also be interpreted as due to a mixture of single-domain (SD) and multidomain (MD) grains [*Dunlop*, 2002]. Comparison with theoretical mixing curves for magnetite [*Dunlop*, 2002] yields a relative amount of MD particles in the mixture varying between approximately 20 and 80% in most cases.

Though useful, information provided by Day-plots can be often ambiguous. Additional information about domain states can be obtained from the shape parameter σ_{HYS} and the coercivity ratio B_{RH}/B_{CR} [*Fabian*, 2003]. Mixtures of fractions with highly contrasting coercivities arising from assemblages of various magnetic components with different mineralogy or grain size may result in shape anomalies of hysteresis loops [e.g., Roberts *et al*., 1995; *Muttoni*, 1995; *Tauxe et al*., 1996]. Shape parameter σ_{HYS} quantifies the shape of the hysteresis loop, with $\sigma_{HYS} > 0$ for wasp-waisted and $\sigma_{HYS} < 0$ for pot-bellied loops. In the present study, shape parameter σ_{HYS} yielded negative values in all but two cases, both belonging to historic volcanic flow TM2 (supporting information Figure S1b). As σ_{HYS} is fairly independent of grain size within the SD-MD region, variations in this parameter point to the presence of SP grains or additional mineral fractions [*Fabian*, 2003]. In supporting information Figure S1b, the latter parameter is plotted against the B_{RH}/B_{CR} ratio. High B_{RH}/B_{CR} ratios indicate large particles, while natural ensembles that contain SP particles display B_{RH}/B_{CR} ratios below 1 [*Fabian*, 2003]. The variation of σ_{HYS} for most samples, except of four belonging to historic volcanic flows TM1, TM2, and TM3 and two to Pleistocene flow LZ12 is not very large, varying between -0.44 and -1.04. Thus, the larger differences in the B_{RH}/B_{CR} ratio of the studied samples should be mostly attributed to their SD-MD trend. However, in the four aforementioned samples belonging to historic lavas, B_{RH}/B_{CR} is smaller than 1, and σ_{HYS} has smaller negative values than those of the remaining samples or even positive values, and may therefore indicate that SP particles or other mineral fractions are present.

5. Paleointensity Results

5.1. Paleointensity Determinations With the *Coe* Method

After analyzing paleomagnetic and rock-magnetic results, 12 out of 16 flows were preselected for paleointensity experiments with the *Coe* [1967] method. This first selection aimed to exclude those sites/samples from the paleointensity experiments characterized by a large viscous overprint as well as samples with an irreversible thermomagnetic behavior at relatively low temperatures. Although site LZ5 was characterized by the presence of relatively large viscous overprints, some samples of that flow displayed a smaller viscous component which could be erased at temperatures below 200°C or fields of 5–8 mT, and these samples were not rejected. Five of the preselected flows were emitted during the historical eruptions in 1731–1736 and 1824 A.D., and seven were Pleistocene flows. Interpretation of paleointensity results was accomplished with the ThellierTool4.0 software [*Leonhardt et al*., 2004]. The reliability of a paleointensity determination depends on the quality of the experimental conditions, the occurrence of alteration, and the presence of remanent magnetization carried by MD grains. Statistical parameters and reliability criteria for paleointensity determinations have been proposed to take into account these experimental conditions [e.g., *Selkin and Tauxe*, 2000; *Kissel and Laj*, 2004; *Paterson et al*., 2014], but no particular criteria and parameter set is generally applied. In the present study, some of the studied rocks belong to historic lava flows, and the field intensity in which magnetization was acquired can be retrieved from models. In such

a case, it can be interesting to relate the deviation of the results obtained from the known field to the strictness of the chosen criteria. For this reason, the selection of successful paleointensity determinations was performed based on sets of criteria of different stringency, assigning to each preliminary successful determination a specific quality level A, B, or C (supporting information Table S1). The following criteria were considered:

a. The number N of aligned points on the Arai plot, without considering data supposed to be produced by viscous magnetization (VRM) acquired in situ. For all quality levels, $N \geq 4$.
b. NRM fraction factor f [*Coe et al*., 1978] calculated for a chosen segment of the NRM-pTRM diagram and referred to the intersection between linear fit and *y* axis, the so-called "true NRM" [*Leonhardt et al*., 2004]. Fraction factor f varied between $f \geq 0.5$ for class A determinations and $f \geq 0.35$ for classes B and C ones.
c. The standard error/absolute slope of the best fit line on the NRM-pTRM diagram (ratio β) varied among $\beta \leq 0.1$ (class A), $\beta \leq 0.12$ (class B), and $\beta \leq 0.15$ (class C).
d. The quality factor q [*Coe et al*., 1978], with ($q = fg/\beta$), varying between $q \geq 2$ (classes A and B) and $q \geq 1$ (class C).
e. δ(CK) [*Leonhardt et al*., 2000] is the TRM-normalized difference between original TRM and the pTRM check at a given temperature. It is similar to the difference ratio DRAT [*Selkin and Tauxe*, 2000], which is normalized to the segment of the Arai plot used for paleointensity determination. It varied among $\delta(CK) \leq 5\%$ (class A), $\delta(CK) \leq 7\%$ (class B), and $\delta(CK) \leq 10\%$ (class C).
f. Directions of NRM end-points obtained in the zero-field steps of the experiment must draw a straight line pointing to the origin in the segment chosen for paleointensity determination. Maximum angular deviation (MAD) of the anchored-to-the-origin fit should be smaller than 7° (class A) or 15° (classes B and C). Furthermore, the angle α between the vector average of the data selected for paleointensity determination (which is anchored to the center of mass of the data) and the principal component of the data (anchored to the origin) should be smaller than 15° for all classes.
g. Arai plots must not have a clearly concave-up shape, because in such cases, remanence is most likely associated with the occurrence of MD grains [*Levi*, 1977]. This was checked by quantification of the curvature k of the selected data points of the Arai plot [*Patterson*, 2011]. For classes A and B, curvature $k \leq 0.164$, a threshold defined using samples with known grain sizes [*Patterson*, 2011], and for class C, $k \leq 0.270$, a possible upper threshold mentioned by *Patterson* [2011], which nonetheless was not supported by all his data. To determine k, the Thellier GUI software [*Shaar and Tauxe*, 2013] was employed.

Though not exactly equal, class A criteria are similar to those proposed by *Kissel and Laj* [2004] or *Leonhardt et al*. [2000] (class A), but with a main difference in the case of fraction factor f, for which we require a more demanding threshold $f \geq 0.5$. Type B criteria would be similar to those proposed by *Selkin and Tauxe* [2000] or *Leonhardt et al*. [2000] (class B), although allowing a slightly higher uncertainty of the best fit line in the Arai-plot. Class C determinations would allow a somewhat larger disparity between original TRM value and pTRM check. In addition, curvature k is taken into account in all three classes. If the aforementioned criteria are used, 43 samples out of 78 analyzed (55.1%) can be included into one of these three classes (supporting information Table S1). Ten (12.8%) belong to class A, 17 (21.7%) to class B, and 16 (20.5%) to class C. Only seven successful determinations yielded a fraction factor f smaller than 0.5, but δ(CK) values were above 7% in 11 cases, giving rise to most class C determinations. Determinations on 35 (44.9%) samples were rejected. Most excluded samples did not fulfill criterion (g), regarding the presence of MD grains, or showed significant alteration. In various cases, scattered Arai plots were obtained which did not allow paleointensity determination. Supporting information Table S2 shows successful paleointensity determinations obtained with the Coe method, Table 2 the corresponding mean flow values, and Figure 5 examples of a successful and a failed paleointensity determination.

5.2. Paleointensity Determinations With the Multispecimen Method

The paleomagnetic behavior of samples from the 12 flows selected for paleointensity experiments was characterized by a single component occasionally accompanied by a soft overprint, and M_S-T curves generally displayed a reversible behavior, with a single phase characterized by a high Curie temperature between approximately 500°C and 575°C. The chosen heating temperature of 450°C appeared suitable to remove

Table 2. Comparison of Mean Paleointensity Results Obtained With the Coe Method and Multispecimen Methods[a]

	Coe Method		MSP-DB(NC)		MSP-DSC(AC)	
SITE	N	Intensity (μT)	N	Intensity (μT)	N	Intensity (μT)
Historical Flows						
TM1	3	40.5 ± 1.9	6	86.9 [79.3-N.A.]	6	43.9 [39.7–46.5]
LZ9	3	38.3 ± 2.3	7	17.4 [11.0–25.5]	5	18.5 [14.0–25.4]
TM3	4	41.9 ± 4.1	6	41.0 [35.6–44.0]	6	22.8 [20.3–29.1]
TM2	5	44.2 ± 6.9	6	32.3[29.8–37.7]	6	21.7 [19.4–28.6]
TM4	4	39.9 ± 4.3	6	43.3 [40.6–46.4]	6	30.7[26.2–33.9]
Pleistocene Flows						
LZ1	6	46.9 ± 3.1	6	35.0 [32.7–38.4]	4	30.7 [26.3–33.4]
LZ4	6	29.4 ± 4.6	4	46.2 ± 4.1		
LZ7	2	27.7 ± 3.3	4	29.3 [25.4–31.3]	4	23.0 [21.0–28.7]
LZ5	1	24.7 ± 0.6	6	24.2 ± 3.5		
LZ10	3	27.3 ± 3.4	7	20.6 [14.3–23.0]	6	12.6 [2.5–17.2]
LZ12	1	27.2 ± 1.4	7	28.6 [14.5–33.4]	7	21.8 [19.8–22.8]
LZ3	5	45.9 ± 5.8	6	45.1 [38.5–49.1]	6	28.8 [23.5–35.4]
Expected Paleointensity						
1731/1732				44.9 ± 0.9		
1736				45.0 ± 0.9		
1824				44.3 ± 0.9		

[a]*N (Coe method)*: number of samples used for calculation of mean paleointensities in each flow. Error is given by standard deviation. In LZ5 (1 sample), paleointensity determination uncertainty is indicated. *N (Multispecimen* [*Dekkers and Böhnel*, 2006] *and domain-state and alignment corrected* [*Fabian and Leonhardt*, 2010]*)*: number of specimens used for calculation of multispecimen paleointensities in each flow. Lower and upper bound of the confidence interval of domain-state corrected samples are indicated. Expected paleointensity values were calculated with model SHA.DIF.14k [*Pavón-Carrasco et al*., 2014].

possible overprints and lay slightly below the lowermost Curie temperature observed in type H curves, so that it was less likely that heating was able to induce thermochemical alteration on the specimens.

Paleointensity results obtained with the multispecimen protocol are shown in supporting information Tables S3a and S3b. As mentioned above, in two flows (LZ4 and LZ5), the original method as proposed by *Dekkers and Böhnel* [2006] (DB) was applied, while in the remaining ones, the extended protocols for fraction correction (FC) and domain-state correction (DSC) [*Fabian and Leonhardt*, 2010] were used. Supporting information Table S3a displays results of the standard, fraction corrected, and domain-state corrected determinations, and supporting information Table S3 shows the alignment-corrected results for these determinations [*Monster et al*., 2015b]. Reliability criteria listed in supporting information Tables S3a and S3b include quality of the linear least squares fit (R^2), an alteration criterion (ε_{alt}), and a check of whether or not the linear regression intersects the *y* axis within the theoretically prescribed limits [*Monster et al*., 2015b]. In flows LZ4 and LZ5 (supporting information Table S3a), the only criterion is the quality of the linear least squares fit. *De Groot et al*. [2013] suggest that $\varepsilon_{alt} \leq 3$.

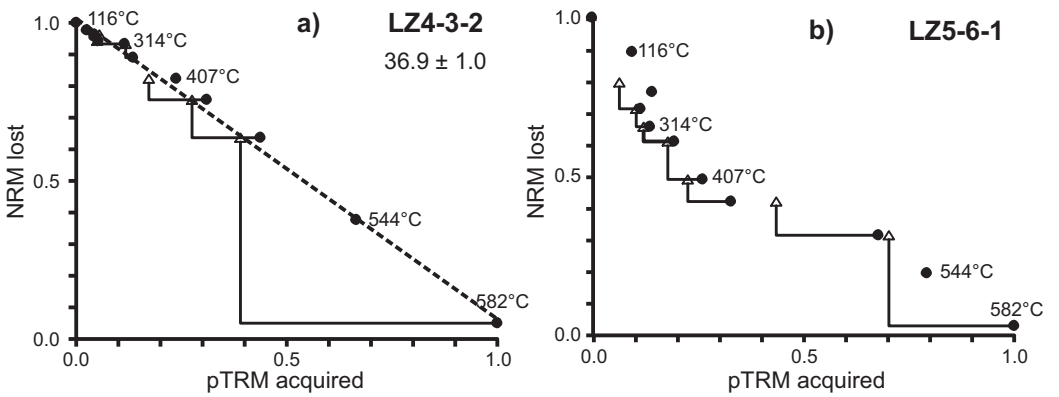

Figure 5. Paleointensity determinations with the Coe method. (a) NRM-TRM plot of successful determination of specimen LZ4-3-2 (Pleistocene flow). All points were used for paleointensity determination. (b) Unsuccessful paleointensity experiment on specimen LZ5-6-1 (Pleistocene flow). Triangles represent pTRM-checks.

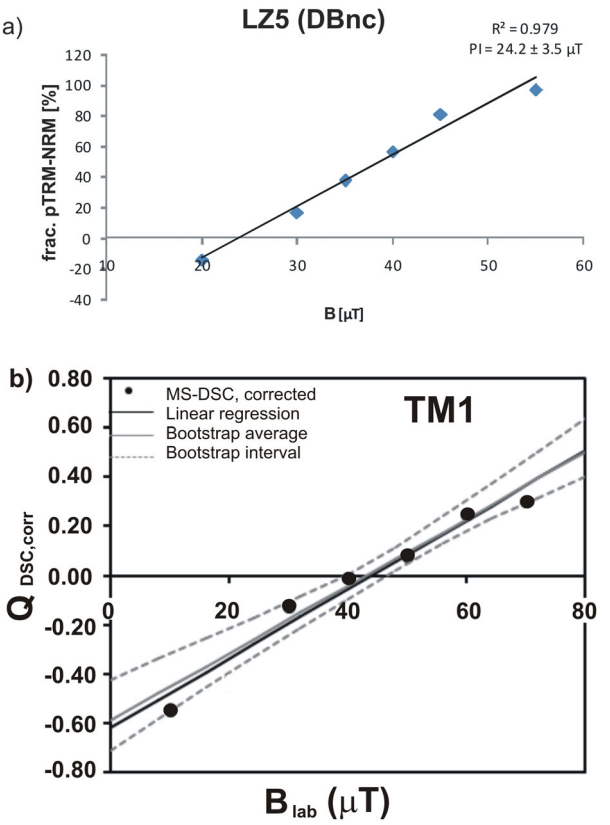

Figure 6. Paleointensity determinations with multispecimen methods. (a) Paleointensity multispecimen determination with the method of *Dekkers and Böhnel* [2006]. Sample LZ5 (Pleistocene flow). *Frac. pTRM-NRM (%)*: Fraction of sample magnetization at different magnetizing fields compared to original NRM; *B*: magnetizing field. (b) Paleointensity multispecimen determination with domain-state correction and alignment correction [*Fabian and Leonhardt*, 2010]. Domain-state and alignment corrected magnetization ratio. *B*: magnetizing field. Sample TM1 (Historical flow). $Q_{DSC,corr}$: figure modified from VBA Software Tool [*Monster et al.*, 2015b].

Fraction and domain-state corrected determinations without alignment correction yield mostly unreliable results. In fact, in most cases, no satisfactory linear regression can be obtained from the data (supporting information Table S3a). However, application of alignment correction greatly improves their linear trend (supporting information Table S3b). However, alteration parameter $\varepsilon_{alt} \leq 3$ is only fulfilled by flows TM2 and LZ3. Linear fits should intersect the *y* axis between (0, −1). Failure to do so may indicate that something besides domain-state-related processes is affecting the paleointensity determination [*Monster et al.*, 2015b] and that the determination might be not reliable. While the greater part of alignment-corrected results from historical flows fulfil this criterion, none of the Pleistocene results do. Both sites studied with the original MS method display a good linear fit with $R^2 > 0.95$. Figure 6 shows examples of paleointensity determinations with the MS method.

In Figure 7a, paleointensity results obtained with the Coe method and the uncorrected Dekkers and Böhnel procedure are shown. These latter data have been chosen as they are equivalent to the original MS method. Figure 7b displays a comparison of results from the Coe method and the domain-state and alignment corrected procedure.

6. Discussion of Results

6.1. Quality of Thellier-Type Paleointensity Results

Expected paleointensity results from the 1730–1736 and 1824 A.D. eruptions were calculated with model SHA.DIF.14k [*Pavón-Carrasco et al.*, 2014], and paleostrength values obtained in the present study from historical flows could be then compared with them. As paleointensity results obtained with the Coe method have been classified into different levels according to certain quality criteria, it might be interesting to analyze the deviation of the results obtained from the known field to the strictness of the chosen criteria. As shown by Table 2 and Figure 7, mean paleointensity values obtained with the Coe method on the historical flows either agree within uncertainty limits with the expected ones or show a slightly lower than expected value (TM4 and TM1). In flow TM3, only class A paleointensity determinations were obtained. In the remaining four historical flows, however, no correlation between quality class and agreement with expected values can be observed (supporting information Figure S2).

As shown in supporting information Figure S1, hysteresis parameter ratios display PSD behavior, and approximately lie on an SD-MD mixing curve for magnetite as calculated by *Dunlop* [2002]. The lower the M_{RS}/M_S and the higher the B_{CR}/B_C ratio, the more pronounced is the tendency toward an MD behavior. Thus, a ratio $QSD = (M_{RS}/M_S)/(B_{CR}/B_C)$ can give a rough picture of the domain structure of the data set, a low value pointing toward MD-behavior, and a high one toward SD characteristics. Supporting information Figure S3 shows that no relation can be observed between MD-behavior, difference between expected and actual paleointensity and quality class of paleointensity determination in historical flows. Supporting

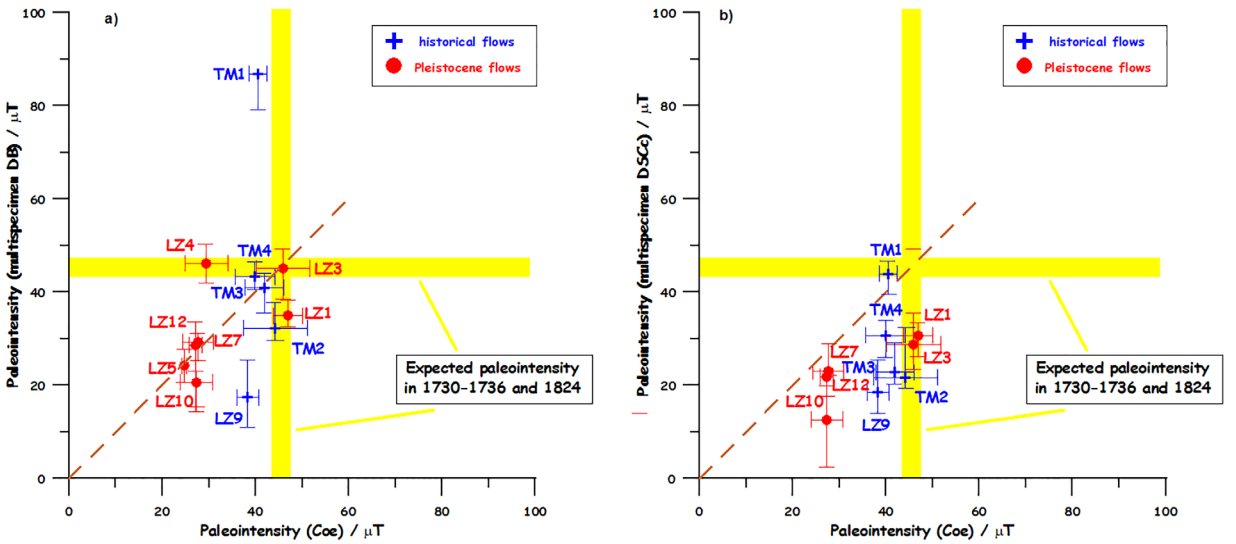

Figure 7. Comparison of paleointensity results obtained with the Coe and multispecimen methods. (a) Comparison between the *Coe* [1967] method and the multispecimen determination method of *Dekkers and Böhnel* [2006]. (b) Comparison between the *Coe* [1967] method and multispecimen determination with domain-state correction and alignment correction [*Fabian and Leonhardt*, 2010]. Results are shown with error bars. Expected palaeointensity results from the 1730–1736 A.D. and 1824 A.D. eruptions calculated with global model SHA.DIF.14k [*Pavón-Carrasco et al*., 2014] are shown with two crossed grey bars. Dashed line at 45° is drawn to identify equality or inequality of results obtained with both methods.

information Figure S4 shows a plot of quality class of paleointensity determinations (including unsuccessful determinations) against QSD ratio and no relation between both parameters can be observed.

6.2. Historical Flows

As shown by Table 2 and Figure 7, mean paleointensity values obtained with the Coe method on the historical flows either agree within uncertainty limits with the expected ones or show a slightly lower than expected value (LZ9 and TM1). Paleointensity results from site TM3, which shows a good agreement, is only based on class A determinations, but this relation cannot be generalized to other flows. On the other hand, the paleointensity obtained in flow TM1 (erupted in 1824 A.D.) displays a small uncertainty and disagrees with the expected one by approximately 10%. Results in this case were obtained from lower quality determinations, but its lower paleointensity could be perhaps also explained with the bias induced by the crustal field [*Valet and Soler*, 1999], due to the extensive volcanism of the 1730–1736 A.D. eruptions, which surrounds this 1824 A.D. flow.

Multispecimen determinations with the uncorrected *Dekkers and Böhnel* [2006] procedure, however, show worse behavior. Two flows (TM3 and TM4) yield the expected results, but site TM2 shows a significant deviation, and paleointensities obtained from flows LZ9 and TM1 display extremely anomalous values (both with a large experimental uncertainty). It might be worth trying to correlate these results with the quality of paleointensity determinations obtained on the same samples with the Coe method. However, no significant correlation is observed, as correct paleointensity values on flow TM3 were obtained on specimens with class A determinations with the Coe method, and those from TM4 from classes B and C determinations. Erroneous results, on the other hand, were attained on classes A, B, and C samples, and only TM1 was based on clearly lower quality determinations (supporting information Table S2).

MS paleointensity results obtained with the fraction-corrected protocol do not differ significantly from those obtained with the uncorrected DB procedure (supporting information Table S3b), but DSC data show a different picture (Figure 7b). In that case, only flow TM1 yields a correct result, but all remaining historical flows display clearly underestimated values. The result of flow TM1 points to an overestimation of the uncorrected MS-determination due to MD behavior, which is corrected by the DSC protocol, although $\varepsilon_{alt} > 3\%$. In flows TM3 and TM4, which displayed correct paleointensities, the underestimated DSC paleointensities may be explained by considerable alteration due to successive heating during the extended MS procedure, but despite absence of alteration a significant paleointensity decrease is also observed in TM2. The deviation from the expected result observed on MS determinations in TM2 does not correlate with the class A correct value obtained with the Coe experiment. The failure of MS paleointensity determinations in LZ9 is difficult

to explain. Type L M_S-T curves of this flow show a reversible behavior at 480°C, and hysteresis parameters show a PSD domain structure not specially biased toward MD behavior. The Thellier-type experiment performed on the same sample yielded, however, a type C determination. It is worth to recall that in none of these cases the individual paleointensity determinations performed on each sample with the Coe method differ significantly from the flow mean.

6.3. Pleistocene Flows

Analysis of paleointensity results on the seven studied Pleistocene flows yields an excellent agreement between the Coe and the MS-DB methods in flows LZ3, LZ5, LZ7, and LZ12, a moderate disagreement in LZ10, and significant disagreements in LZ1 and LZ4 (Table 2 and Figure 7a). Nonetheless, if agreement of results obtained with both methods is considered an indicator of correct determinations, as might be suggested by the results attained on historical flows, no clear correlation arises between them and paleointensity determination quality or rock-magnetic properties. In fact, only in flows LZ5 and LZ10, a class A determination could be obtained. Samples from flows LZ3 and LZ10 show PSD domain structure in hysteresis curves with a slight bias toward SD behavior in the latter case. The paleointensity result with the Coe method in site LZ5 is based on a single type A determination, as all other experiments led to rejection because of concave-up-shaped Arai plots due to MD-behavior and alteration. Hysteresis measurements provided PSD grain sizes with more or less developed MD characteristics. In this case, the MS-DB experiment seemed to be capable to produce similar paleointensity results as the one obtained with the Coe method, although it had been performed on a sister specimen of a sample which yielded a failed paleointensity determination with the Coe method because of MD behavior. Similarly, because of the same reason as well as alteration at higher temperatures, the sample from flow LZ7 used for multispecimen experiments yielded no paleointensity results in the Coe experiment. In this case, MD behavior was additionally confirmed by hysteresis data. However, the multispecimen method seemed in this case capable to produce the same paleointensity result than the mean of the two successful Thellier-type determinations of site LZ7. Hysteresis measurements of LZ12 samples yield PSD grain sizes with a clear MD tendency.

Results from the remaining flows LZ1 and LZ4 are more difficult to interpret. If Thellier-type determinations are considered by themselves, six out of eight type B and C determinations in flow LZ1, and six out of six mostly type B determinations in flow LZ4 point to successful paleointensity determinations in both cases, as the ratio of the standard deviation of the field estimates to the intensity average is clearly lower than 25%, a limit proposed by *Selkin and Tauxe* [2000] to consider paleofield estimates reliable. These results disagree, nevertheless, with those obtained from MS experiments. In site LZ4, hysteresis parameters show PSD behavior with a strong MD bias. This MD behavior could have led to an overestimation of the MS determination, as predicted by *Fabian and Leonhardt* [2010]. This again poses the question of why this MD behavior has led to a successful (though lower quality) type C paleointensity determination with the Coe method on the same sample or why in some cases, as also shown in the present study, acceptable paleointensity estimates are attained with the MS-DB method on samples clearly affected by MD behavior. Regarding discordant multispecimen and Thellier-type results in flows LZ1 and LZ4, it would be interesting to have the support of more than one multispecimen determination per studied site. Comparison of Thellier-type and MS-DSC paleointensity results shows a pronounced disagreement in all flows except in LZ7, where results agree within error limits (no MS_DSC data were available for flows LZ4 and LZ5). In three cases, this behavior might be explained by the occurrence of alteration during the expanded MS procedure (LZ1, LZ10, and LZ12). However, flow LZ7 displays the highest ε_{alt} value while LZ3 shows no alteration at all (supporting information Figure S3b).

6.4. Mean Paleointensity Results

In all studied flows, the ratio of the standard deviation of the field estimates obtained with the Coe method to the intensity average was clearly lower than 25% (Table 2), although in flows LZ5 and LZ12, this criterion was not taken into account because only a single determination was available. As a result, a mixed data set was obtained in which for each flow both Thellier-type and a multispecimen paleointensity determination were available. As discussed above, in certain cases, a good agreement between both methods was observed, while in other cases, significant differences appeared, posing the question about which results reflect the actual paleointensity value in the case of nonhistorical flows.

Table 3. Mean Paleointensity Results and Virtual Axial Dipole Moments (VADM)[a]

Flow	N(n/MS)	Paleointensity (μT)	VADM (10^{22}Am^2)
Historical Flows			
1824	1 (3/1)	41.4 ± 2.3	8.20 ± 0.06
1731–1736	4 (16/2)	40.2 ± 1.7	8.0 ± 0.3
Pleistocene Flows			
LZ1	1 (6/0)	46.9 ± 3.1	9.4 ± 0.6
LZ4	1 (6/0)	29.4 ± 4.6	5.8 ± 0.9
LZ5	1(1/1)	24.5 ± 0.4	4.85 ± 0.08
LZ7	1(2/1)	28.2 ± 2.5	5.6 ± 0.5
LZ12	1(1/1)	27.9 ± 1.0	5.5 ± 0.2
LZ3	1(5/1)	45.8 ± 5.2	9.1 ± 1.0

[a]*N(n/MS): N*: number of flows used for calculation of mean paleointensities; *n*: number of determinations performed with the Coe method on individual specimens used for calculation of mean paleointensities; *MS*: number of multispecimen determinations used for calculation of mean paleointensities (for explanation, see text)

All except one of the historical flows analyzed in the present study belong to the 1730–1736 A.D. eruptions. These four flows either yielded the expected paleointensity or a near value with the Coe method. The MS-DB provided two determinations agreeing with the expected intensity, and one moderately deviated determination (Table 2). Taking advantage of the fact that historical flows allow the comparison of the results obtained with those predicted by models, all paleointensity results which agreed with the models were taken into account. This procedure led to discard the moderately deviated MS determination from TM2 and the extremely diverging determination from LZ9. A mean paleointensity was calculated for each flow combining the single multispecimen result (if available) with all successful Thellier-type data of each flow. Thus, the multispecimen determination was given the same weight as an individual Thellier-type determination, as the former is based on an experiment performed on a single sample of each flow. Subsequently, a mean of all four flows from the 1730–1736 A.D. eruption was calculated. The Thellier-type and MS-DSC determinations on 1824 flow TM1 agree with the expected value and therefore the paleointensity value obtained is based on three determinations with the Coe method and the MS-DSC.

In the case of the Pleistocene flows, one of the two following criteria had to be fulfilled in order to deem a flow result reliable: (i) coincidence of paleointensity results obtained with both methods or (ii) a paleointensity result based on a sufficiently large number ($n > 4$) of individual Thellier-type determinations. As no coincidence of paleointensity results was observed between the Coe and the MS-DSC methods except in flow LZ7, and the latter site was characterized by considerable alteration, Thellier-type results were only combined with MS-DB determinations. Application of the aforementioned criteria lead to the rejection of flow LZ10, where only three samples yielded successful determinations with the Coe method, and the paleointensity obtained did not agree with the multispecimen determination.

Mean paleointensity results are shown in Table 3 together with virtual axial dipole moments (VADM). In most Pleistocene flows, a relatively weak VADM around 5×10^{22} Am^2 was observed, although two flows display higher values around 9×10^{22} Am^2. Historical flows yield VADMs around 8×10^{22} Am^2. Some new paleointensity data from historical and Holocene lavas from the Canary Islands have been recently published. *Kissel et al*. [2015] studied 37 historical to Holocene flows from Gran Canaria and Tenerife with the original *Thellier and Thellier* [1959] method, obtaining VADMs between 5 and 16×10^{22} Am^2, with a prominent paleointensity peak around 600 B.C. *De Groot et al*. [2015] applied a multimethod paleointensity approach to 19 lavas from Gran Canaria and Tenerife dating between 4000 B.C. and 1909 A.D. Their VADMs vary between approximately 6 and 16×10^{22} Am^2, and they also observe a paleointensity peak around 700 B.C. *Monster et al*. [2015a] performed a multimethod paleointensity study on nine flows from La Palma on historical and Holocene age ($\leq$3.2 ka) and VADMs vary between 6 and $10 \cdot \times 10^{22}$Am^2.

7. Conclusions

A rock-magnetic, paleomagnetic, and paleointensity study was performed on 16 lava flows of Miocene, Pleistocene, and historical age from Lanzarote (Canary Islands, Spain) with two main goals: (i) compare paleointensity results obtained with two different techniques and (ii) obtain new paleointensity data. Paleointensity determinations were carried out with a Thellier-type method as modified by *Coe* [1967] and with the multispecimen method [*Dekkers and Böhnel*, 2006; *Fabian and Leonhardt*, 2010], and both methods were applied on sister specimens of the same samples.

After analyzing paleomagnetic and rock-magnetic results obtained, 12 out of 16 flows were chosen for paleointensity experiments. A selection of successful paleointensity determinations was performed based on

sets of criteria of different stringency. In such way, the quality of the paleointensity results obtained could be compared to the strictness of the chosen criteria, as part of the studied rocks belonged to historical lava flows with magnetization acquired in a field which could be retrieved from models. Paleointensity values obtained with the Coe method on the historical flows either agree within uncertainty limits with the expected ones or show a moderately lower than expected value. Multispecimen determinations, on the other hand, show worse agreement, as one site shows a significant deviation from the expected result and two other flows display extremely anomalous values. Nevertheless, no clear relation can be detected between correct or anomalous results, rock-magnetic characteristics or paleointensity determination quality class. Results on historical flows suggest that agreement between results from both methods seems to be, on the other hand, a good indicator of correct paleointensity determinations

Comparison of paleointensity results obtained with both methods on the seven studied Pleistocene flows yields an excellent agreement in four cases, a relatively small disagreement in one case and significant disagreements in two more cases. Nonetheless, if agreement of results obtained with both methods is considered an indicator of successful determinations, as suggested by the results attained on historical flows, again no clear correlation arises between them and paleointensity determination quality or rock-magnetic properties.

The use of the extended MS protocol as proposed by *Fabian and Leonhardt* [2010] includes a procedure to avoid paleointensity overestimates due to samples containing a significant MD fraction and provides criteria to better assess the reliability of paleointensity determinations obtained. However, it includes an extra number of heating steps which may lead to alteration, as probably happened to several samples in the present study. Therefore, caution must be exerted when choosing the most reliable results provided by the extended MS protocol.

A mean paleointensity has been calculated for the flows belonging to the 1730–1736 eruptions averaging Thellier-type and multispecimen data, giving the same weight to a multispecimen determination as to an individual Thellier-type determination. The same procedure was applied to the 1824 flow. In nonhistorical flows in certain cases, a good agreement between Thellier-type and multispecimen methods was observed, while in other cases, significant differences appeared, so that the question arises about which results reflect the actual paleointensity value. It was decided that in the case of the Pleistocene flows, one of the two following criteria had to be fulfilled in order to deem a flow result reliable: (i) coincidence of paleointensity results obtained with both methods or (ii) a paleointensity result based on a sufficiently large number of individual Thellier-type determinations. Application of these criteria led to the rejection of the results of one flow.

Acknowledgments
This work was funded by project CGL2012-32149 (*Ministerio de Economía y Competitividad*, Spain), project 320/2011 (*Ministerio de Medio Ambiente y Medio Rural y Marino*, Spain) and the European Regional Development Fund (ERDF). We especially wish to thank Orlando Hernández and Jaime Arranz (*Casa de los Volcanes, Cabildo de Lanzarote*) for their help during our fieldwork in Lanzarote. We also wish to thank three anonymous reviewers for their useful and constructive comments and suggestions. The data used in this work are listed in the tables and references.

References

Abdel-Monem, A., A. N. D. Watkins, and P. W. Gast (1971), Potassium-Argon ages, volcanic stratigraphy an geomagnetic polarity history of the Canary Islands: Lanzarote, Fuerteventura, Gran Canaria and La Gomera, *Am. J. Sci.*, 490–521.

Anguita, F., and F. Hernán (2000), The Canary Islands origin: A unifying model, *J. Volcanol. Geotherm. Res.*, *103*, 1–26.

Besse, J., and V. Courtillot (2002), Apparent and true polar wander and the geometry of the geomagnetic field over the last 200 Myr, *J. Geophys. Res.*, *107*(B11), 2300, doi:10.1029/2000JB000050.

Biggin, A. J., A. McCormack, and A. Roberts (2010), Paleointensity database updated and upgraded, *Eos Trans. AGU*, *91*(2), 15, doi:10.1029/2010EO020003.

Blanco-Montenegro, I., F. G. Montesinos, A. García, R. Vieira, and J. J. Villalaín (2005), Paleomagnetic determinations on Lanzarote from magnetic and gravity anomalies: Implications for the early history of the Canary Islands, *J. Geophys. Res.*, *110*, B12102, doi:10.1029/2005JB003668.

Böhnel, H., M. J. Dekkers, L. A. Delgado-Argote, and M. N. Gratton (2009), Comparison between the microwave and the multispecimen parallel difference pTRM paleointensity methods, *Geophys. J. Int.*, *17*(2), 383–394.

Bol'shakov, A. S., and V. V. Shcherbakova (1979), A thermomagnetic criterion for determining the domain structure of ferrimagnetics, *Izv. Akad. Nauk. SSSR*, *15*, 111–117.

Bowles, J. A., M. J. Jackson, T. S. Berquó, P. A. Sølheid, and J. S. Gee (2013), Inferred time- and temperature-dependent cation ordering in natural titanomagnetites, *Nat. Commun.*, *4*, 1916, doi:10.1038/ncomms2938.

Calvo, M., M. Prévot, M. Perrin, and J. Riisager (2002), Investigating the reasons for the failure of paleointensity experiments: A study on historical lava flows from Mt. Etna, *Geophys. J. Int.*, *149*, 44–63.

Carracedo, J. C., and E. Rodríguez Badiola (1993), Evolucióngeológica y magmática de la isla de Lanzarote (Islas Canarias), *Rev. Acad. Canar. Cienc.*, *V*(4), 25–28.

Carracedo, J. C., E. Rodríguez Badiola, and V. Soler (1992), The 1730-1736 eruption of Lanzarote, Canary Islands: A long, high-magnitude basaltic fissure eruption, *J. Volcanol. Geotherm. Res.*, *53*, 239–250.

Carracedo, J. C., S. Day, H. Gillou, E. Rodríguez, J. A. Canas, and F. J. Pérez (1998), Hotspot volcanism close to a passive continental margin, *Geol. Mag.*, *135*, 591–604.

Chadima, M., and F. Hrouda (2006), Remasoft 3.0 a user-friendly paleomagnetic data browser and analyser, *Travaux Géophys., XXVII*, 20–21.
Coe, R. (1967), Paleointensities of the Earth's magnetic field determined from Tertiary and Quaternary rocks, *J. Geophys. Res., 72*, 3247–3262.
Coe, R., S. Grommé, and E. A. Mankinen (1978), Geomagnetic paleointensities from radiocarbon-dated lava flows on Hawaii and the question of the Pacific nondipol low, *J. Geophys. Res., 83*, 1740–1756.
Coello, J., J. M. Cantagrel, F. Hernán, J. M. Fúster, E. Ibarrola, E. Ancochea, C. Casquet, C. Jamond, J. R. Díaz de Terán, and A. Cendrero (1992), Evolution of the eastern volcanic ridge of the Canary Islands based on new K-Ar data, *J. Volcanol. Geotherm. Res., 53*, 251–274.
Day, R., M. Fuller, and V. A. Schmidt (1977), Hysteresis properties of titanomagnetites: Grain-size and compositional dependence, *Phys. Earth Planet. Inter., 13*, 260–267.
De Groot, L. V., A. J. Biggin, M. J. Dekkers, C. G. Langereis, and E. Herrero-Bervera (2013), Rapid regional perturbations to the recent global geomagnetic decay revealed by a new Hawaiian record, *Nat. Commun., 4*, 2727, doi:10.1038/ncomms3727.
De Groot, L. V., A. Béguin, M. E. Kosters, M. van Rijsingen, E. L. M. Struijk, A. J. Biggin, E. A. Hurst, C. G. Langereis, and M. J. Dekkers (2015), High paleointensities for the Canary Islands constrain the Levant geomagnetic high, *Earth Planet. Sci. Lett., 419*, 154–167, doi:10.1016/jepsl.2015.03.020.
Dekkers, M. J., and H. N. Böhnel (2006), Reliable absolute palaeointensities independent of magnetic domain state, *Earth Planet. Sci. Lett., 284*, 508–517.
Donadini, F., K. Korhonen, P. Riisager, and L. J. Pesonen (2006), Database for Holoecene geomagnetic intensity information, *Eos Trans. AGU, 87*(14), 92–93.
Dunlop, D. (2002), Theory and application of the Day plot (Mrs/Ms versus Hcr/Hc): 1. Theoretical curves and tests using titanomagnetite data, *J. Geophys. Res., 107*(B3), doi:10.1029/2001JB000486.
Fabian, K. (2003), Some additional parameters to estimate domain state from isothermal magnetization measurements, *Earth Planet. Sci. Lett., 213*, 337–345.
Fabian, K., and R. Leonhardt (2010), Multi-specimen absolute paleointensity determination: An optimal protocol including pTRM normalization, domain-state correction and alteration test, *Earth Planet. Sci. Lett., 297*, 84–94.
Fúster, J. M., S. Fernández Santín, and J. Sagredo (1968), *Geology and Volcanology of the Canary Islands, Lanzarote*, 177 pp., Inst. Lucas Mallada, C.S.I.C., Madrid.
Grommé, C. S., T. L. Wright, and D. L. Peck (1969), Magnetic properties and oxidation of iron-titanium oxide minerals in Alae and Makaopuhi lava lakes, Hawaii, *J. Geophys. Res., 74*, 5277–5249.
Hoernle, K. A., and H. U. Schmincke (1993), The role of partial melting in the 15-Ma geochemical evolution of Gran Canaria: A blob model for the canary hotspot, *J. Petrol., 34*, 599–626.
Kirschvink, J. L. (1980), The least-square line and plane and the analysis of paleomagnetic data, *Geophys. J. R. Astron. Soc., 62*, 699–718.
Kissel, C., and C. Laj (2004), Improvements in procedure and paleointensity selection criteria (PICRIT-03) for Thellier and Thellier determinations: Application to Hawaiian basaltic long cores, *Phys. Earth Planet. Inter., 147*, 155–169.
Kissel, C., C. Laj, A. Rodŕguez-González, F. Pérez-Torrado, and J. C. Carracedo (2015), Holocene geomagnetic field intensity variations: Contribution from the low latitude Canary Islands site, *Earth Planet. Sci. Lett., 430*, 178–190.
Korhonen, K., F. Donadini, P. Riisager, and L. J. Pesonen (2008), GEOMAGIA50: An archeointensity database with PHP and MySQL, *Geochem. Geophys. Geosyst., 9*, Q04029, doi:10.1029/2007GC001893.
Kosterov, A., and M. Prévot (1998), Possible mechanisms causing failure of Thellier palaeointensity experiments in some basalts, *Geophys. J. Int., 134*, 554–572.
Leonhardt, R. (2006), Analyzing rock magnetic measurements; The RockMagAnalyzer 1.0 software, *Comput. Geosci., 32*, 1420–1431.
Leonhardt, R., F. Hufenbecher, F. Heider, and H. Soffel (2000), High absolute paleointensity during a mid-Miocene excursion of the Earth's magnetic field, Earth *Planet. Sci. Lett., 184*(1), 141–154.
Leonhardt, R., C. Heunemann, and D. Krása (2004), Analyzing absolute paleointensity determinations: Acceptance criteria and the software ThellierTool4.0, *Geochem. Geophys. Geosyst., 5*, Q12016, doi:10.1029/2004GC000807.
Levi, S. (1977), The effect of magnetite particle size in paleointensity determinations of the geomagnetic field, *Phys. Earth Planet. Inter., 13*, 245–249.
Marinoni, L. B., and G. Pasquarè (1994), Tectonic evolution of the emergent part of a volcanic ocean island: Lanzarote, Canary Islands, *Tectonophysics, 239*(1–4), 111–137, doi:10.1016/004051951(94)9011054.
Michalk, D., A. R. Muxworthy, H. Böhnel, J. MacLennan, and N. R. Nowaczyk (2008), Evaluation of the multispecimen parallel differential pTRM method: A test on historical lavas from Iceland and Mexico, *Geophys. J. Int., 173*, 409–420.
Michalk, D. M., A. J. Biggin, M. F. Knudsen, H. N. Böhnel, N. Nowaczyk, S. Ownby, and M. López-Martínez (2010), Application of the multispecimen palaeointensity method to Pleistocene lava flows from the Trans-Mexican Volcanic Belt, *Phys. Earth Planet. Inter., 179*(3-4), 139–156.
Monster, M. W. L., L. V. de Groot, A. J. Biggin, and M. J. Dekkers (2015a), The performance of various palaeointensity techniques as a function of rock-magnetic behaviour—A case study for La Palma, *Phys. Earth Planet. Inter., 242*, 36–49.
Monster, M. W. L., L. V. de Groot, and M. J. Dekkers (2015b), MSP-Tool: A VBA-based software tool for the analysis of multispecimen paleointensity data, *Frontiers Earth Sci., 3*, 86, doi:10.3389/feart.2015.00086.
Morgan, W. J. (1983), Hotspot tracks and the early rifting of the Atlantic, *Tectonophysics, 94*, 123-139.
Muttoni, G. (1995),Wasp-waisted hysteresis loops from a pyrrothite and magnetite-bearing remagnetized Triasssic limestone, *Geophys. Res. Lett., 22*, 3167–3170.
Pavón-Carrasco, F. J., M. L. Osete, J. M. Torta, and A. De Santis (2014), A geomagnetic field model for the Holocene base don archaeomagnetic and lava flow data, *Earth Planet. Sci. Lett., 388*, 98–109.
Paterson, G. (2011). A simple test for the presence of multidomain behavior during paleointensity experiments. *J. Geophys. Res., 116*, B10104, doi: 10.1029/2011JB008369.
Paterson, G. A., L. Tauxe, A. J. Biggin, R. Shaar, and L. C. Jonestrask (2014), On improving the selection of Thellier-type paleointensity data, *Geochem. Geophys. Geosyst., 15*, 1180–1192, doi:10.1002/2013GC005135.
Roberts, A. P., Y. L. Cui, and K. L. Verosub (1995), Wasp-waisted hysteresis loops: Mineral magnetic characteristics and discrimination of components in mixed magnetic systems, *J. Geophys. Res., 100*(B9), 17,909–17,924.
Roest, W. R., J. J. Dañobeitia, J. Verhoef, and B. J. Collette (1992), Magnetic anomalies in the Canary Basin and the Mesozoic evolution of the Central North Atlantic, *Mar. Geophys. Res., 14*, 1–24.
Schmincke, H. U. (1973), Magmatic evolution and tectonic regime in the Canary, Madeira and Azores islands groups, *Geol. Soc. Am. Bull., 84*, 633–648.
Selkin, P., and L. Tauxe (2000), Long-term variations in palaeointensity¸ *Philos. Trans. R. Soc. London, 358*, 1065–1088.

Shaar, R., and L. Tauxe (2013). Thellier GUI: An integrated tool for analyzing paleointensity data from Thellier-type experiments. *Geochem. Geophys. Geosyst.*, *14*, 677–692, doi:10.1002/ggge.20062.

Shaskanov, V. A., and V. V. Metallova (1972), Violation of Thellier's law for partial thermoremanent magnetizations [in Russian], *Izv. Phys. Solid Earth*, *8*, 180–184.

Soler, V., and J. C. Carracedo, and F. Heller (1984), Geomagnetic secular variation in historical lavas from the Canary Islands, *Geophys. J. R. Atron. Soc.*, *78*, 313–318.

Tauxe, L., T. A. T. Mullender, and T. Pick (1996), Potbellies, wasp-waists, and superparamagnetsim in magnetic hysteresis, *J. Geophys. Res.*, *101*, 571–583.

Thellier, E., and O. Thellier (1959), Sur l'intensité du champ magnétique terrestre dans le passé historique et géologique, *Ann. Geophys.*, *15*, 285–376.

Valet, J. P., and V. Soler (1999), Magnetic anomalies of lava fields in the Canary islands. Possible consequences for paleomagnetic records, *Phys. Earth Planet. Inter.*, *115*, 109–118.

Watkins, N. D., A. Richardson, and R. G. Mason (1966), Paleomagnetism of the Macaronesian Region: The Canary Islands, *Earth Planet. Sci. Lett.*, *1*, 225–231.

Worm, H. U., M. Jackson, P. Kelso, and S. K. Banerjee (1988), Thermal demagnetization of partial thermoremanent magnetization, *J. Geophys. Res.*, *93*, 12,196-12,204.